Environmental Resources Research
Vol. 7, No. 2, 2019

GUASNR

Impacts of climate change on rainfall indices estimation in western sub-basins of Iran

H. Nazaripouya*
Assistant Professor of Watershed Department, Hamedan Agricultural and Natural Resources Research and Education Center, Agricultural Research, Education and Extension Organization, Hamedan, Iran

Received: January 2019 ; Accepted: November 2019

Abstract
The purpose of this study was to document changes in indices simulated by the ensemble application of Coupled Model Inter-comparison Project CMIP5 and CMIP3 when analyzing impacts of climate change on catchment rainfall indices in sub-basins of Hamedan province, west of Iran. The analysis of the precipitation indices consisted of simple rainfall intensity, very heavy rainfall days, maximum one-day rainfall, and rainfall frequency. I investigated the relative change in three rainfall indices based on general circulation models (GCMs) under a mixture of greenhouse gas emission scenarios A1B and B1, RCP8.5 and RCP8.5 for two future periods 2020–2045 and 2045-2065. Results showed that each of the rainfall indices differed in stations under the three GCMs models (GIAOM, MIHR, MPEH5) and emission scenarios A1B, B1, RCP2.5, and RCP8.5. Relative 50y change for future periods 2046–2065 varied from -9.93% to 25% for daily intensity index, from 20.71% to 25.9% for very heavy rainfall days and from -15.71% to 13% for annual rainfall depth in the study area. Rainfall indices projection of sum of wet days, days>1mm, and maximum one-day rainfall showed decrease under the scenarios B1 and A1B and also sum of wet days, simple daily intensity, and heavy rainfall days>10 decreased under the RCP2.6.

Keywords: Climate change, Rainfall indices, Uncertainty, LARS-WG, Hamedan province

*Corresponding author; hnpoya@yahoo.com

Introduction

We can expect strong impact of changes in climate and especially in rainfall on ecosystems as a whole and their components. Diminishing rainfall or increasing dry periods can negatively affect crop yields. On the other hand, increasing downpour, especially during the dry season, can have a positive effect on staple crops as their cultivation period gets extended. CMIP5 or the Coupled Model Intercomparison Project Phase 5 offers a framework for coordinated climate change experiments for the next several years based on which we can simulate and assess climatic conditions (Taylor et al., 2012). CMIP5 focuses on a set of experiments that include higher spatial resolution models, improved model physics, and a more lavish set of output fields (Gulizia and Camilloni, 2015; Taylor et al., 2012).

In the CMIP5 climate change projections, series of emissions and concentrations from the representative concentration pathways (RCPs) described in Moss et al. (2010) are used. Accordingly, general circulation models (GCMs) produced based on CMIP5 have been widely applied in climate change assessment (Gulizia and Camilloni, 2015; Pierce et al., 2013; Smith et al., 2013). Figure 1 depicts the progress of carbon dioxide (CO2) concentrations, as observed in the 20th century and prescribed in the 21st-century simulations in the SRES and RCP scenarios used in this study.

The SRES scenarios are based on the storylines that assume various political, socioeconomic and technological developments causing specified changes in emissions that in turn determine the resulting changes in the atmospheric greenhouse gas concentrations (e.g., Figure 1) and radiative forcing. At the end of the 21st century, the CO2 concentrations can reach approximately 840 ppm in the SRES A2 scenario, 700 ppm in the A1B scenario, and 540 ppm in the B1 scenario which assumes the most environmentally friendly development pathway. As opposed to the SRES scenarios, the radiative forcing trajectories in the RCPs are not linked with predefined storylines and they can mirror a choice of possible combinations of economic, technological, demographic, and policy developments (Moss et al., 2010).

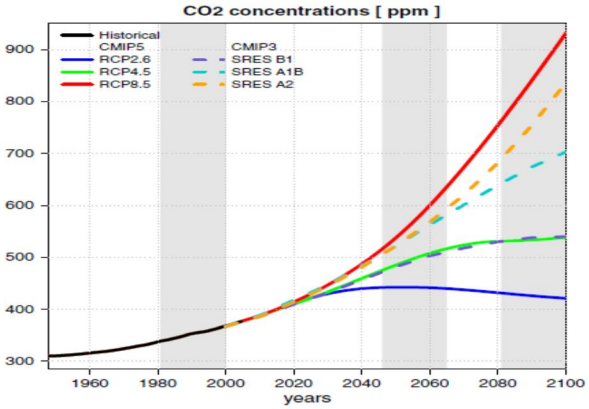

Figure 1. Carbon dioxide (CO2) concentrations in ppm as used in the CMIP3 and CMIP5 historical and scenario simulations and available for download at the PCMDI website. The vertical grey area shows the reference period (1981– 2000) and the two 20 year periods (2046–2065 and 2081–2100) considered in the analysis of future climate change. (J. Sillmann et al., 2016).

The up and down in the RCP2.6 scenario is designed to meet the 2°C global average warming target compared to pre-industrial conditions (van Vuuren et al., 2011a). This scenario has a peak in the radiative forcing at approximately 3 W/m2 (~400 ppm CO2) before 2100 and then falls to 2.6 W/m2 by the end of the 21st century (~330 ppm CO2). Radiative forcing in the RCP4.5 scenario culminates at approximately 4.5 W/m2 (~540 ppm CO2) in the year 2100 (Thomson et al., 2011). RCP4.5 is similar to the SRES scenario B1 with similar CO2 concentrations, and median temperature rises

by 2100 according to Rogelj et al. (2012). RCP8.5 assumes a high rate of radiative forcing augmentation, peaking at 8.5 W/m2 (~940 ppm CO2) in the year 2100 Riahi et al., 2011.

We cannot directly compare climate changes simulated in the CMIP3 and CMIP5 ensembles as the prescribed forcing agents (e.g., CO2 and aerosols) between the SRES and RCP scenarios are different (Rogelj et al., 2012). So, the models may respond differently to a specific radiative forcing due to dissimilar model-specific climate sensitivities.

Using the underlying radiative forcing (or CO_2 concentrations), however we can contrast projected changes in the precipitation indices and provide an estimate of uncertainty of different emission scenarios. The occurrence of extreme rainfall events is one of the most significant aspects of climate. The increase in frequency and intensity of extreme rainfall events may bring about major impacts on natural and man-made systems in terms of increased frequency and severity of floods. For many regions in the world, the frequency and intensity of heavy rainfall events have increased over the past 50 years (Frich et al., 2002; IPCC, 2007). In this regards, it was projected that we may have more severe wet extremes in many areas where mean rainfall were expected to increase, and more severe dry extremes in areas where mean rainfall were projected to decrease (IPCC 2007). This is particularly important for watersheds where runoff from extreme rainfall amount events causes rising streamflows (Zhang et al., 2008; Kwon et al., 2011). However, for better disaster management and mitigation, it is more important to understand the changes in the extremity of weather measures rather than the changes in mean pattern. Therefore, we require knowing the magnitudes of extreme rainfall events over various parts of the world and sub-basins in Hamedan Province West of Iran are no exception. Most studies point to the fact that future climate changes may lead to rises in climate variability and the frequency and intensity of extreme events. Various researchers investigated the frequency and magnitude of extreme rainfall, both at global and at regional scales under the enhanced greenhouse conditions (e.g., Palmer and Ra is a ¨nen, 2002; Watterson and Dix, 2003; Meehl et al., 2005). Many GCMs results consistently predict increases in the frequency and magnitudes of extreme climate events and unevenness of rainfall (IPCC, 2007). Rutger Dankers & Roland Hiederer (2008) showed that on rainy days, the intensity and variability of the precipitation undergoes a general rise, even in areas that are getting much drier on average.

Guhathakurta (2011) showed the frequency of heavy downpour events is decreasing in significant parts of central and north India while they are increasing in peninsular, east and, northeast India. He also demonstrated that extreme rainfall and flood risk are increasing significantly in the country except for some parts of central India. Nazaripouya et al. (2016) evaluated the uncertainties of climate change impacts on temperature, rainfall and runoff in the Ekbatan Dam watershed by CMIP3 models for the 2045-2065 period.

Andreas Haensler et al. (2013) assessed the CMIP3 and CMIP5 databases, along with some recently downscaled regional CORDEX Africa projections and concluded that independent of the underlying emission scenario, annual total rainfall amounts over the central African region are not likely to change severely in the future. Also, they projected that some robust changes would happen in rainfall features such as the intensification of heavy rainfall events and increase in the number of dry spells during the rainy season.

Seree Supharatid et al. (2015) studied CMIP3-CMIP5 climate models rainfall projection and implication of flood vulnerability for Bangkok and concluded that the multi-model mean shows continuous rise in the rainfall from the near future to the far future while the multi-model median shows bigger rainfall only for the distant future.

Saeed et al. (2013) studied the reasons for the opposite climate change signals in rainfall between the regional climate model REMO and its driving earth system model MPI-ESM over the greater Congo region.

Three REMO simulations following three RCP scenarios (RCP 2.6, RCP 4.5 and RCP 8.5) were conducted, and they found opposite signals with REMO showing a decrease and an increase with MPI-ESM in the future rainfall, which diverged strongly from a less extreme to a more extreme scenario. Zhouet et al. (2014) projected changes in temperature and precipitation extremes in China for the end of the twenty-first century based on CMIP5 simulations. The temporal changes and their spatial patterns were analyzed in the Expert Team on Climate Change Detection and Indices (ETCCDI) indices under the RCP4.5 and RCP8.5 emission scenarios. They projected substantial changes in temperature and precipitation extremes under both emission scenarios as compared to the reference period 1986–2005.

Anil Acharya (2013) demonstrated that the cumulative annual rainfall for every 30 years shows a nonstop reduction from 2011 to 2099; however, the summer convective storms which are considered as extreme storms are expected to be more intense in future.

Ray et al. (2000) conducted a trend analysis of heavy rainfall events over selected stations all over India and reported a diminishing trend over most parts of the country. In some other studies, the extreme precipitation projections have shown the highest rise in the rainfall intensity for the most intense storms (i.e., extreme short-duration storms) (Ra insane and Joelsson, 2001; Buonomo et al., 2007). Pourtouiserkani et al. (2014) studied climate change impact on the extreme rainfall for Chenar-Rahdar basin, Fars, Iran using two AOGCM model outputs (HadCM3 and CGCM3) which were downscaled from monthly to daily for the future period of the 2020s (2011-2040) using statistical downscaling techniques including change factor, LARS-WG, SDSM, and, weather generator stochastic methods. Based on the downscaled rainfall time series, the maximum 24-hour precipitation for the two AOGCM models was extracted and then frequency analyses were performed to obtain future daily rainfalls with different return periods. When the three downscaling techniques were compared, the researchers found that change factor and LARS-WG methods were conservative enough for climate change impact assessment for the next 30 years.

Yue-Ping Xu et al. (2012) examined the likely impact of climate change on extreme rainfall in the Qiantang River Basin for three future periods 2011–2030, 2045-2065 and 2080–2099. They also assessed the uncertainty in the evaluation using the three GCMs models and three emission scenarios. Results showed that the 24-h rainfall depth rises in most of the stations under the three GCMs and emission scenarios and there are large uncertainties in the estimations of 24-h rainfall depths at seven stations attributable to GCMs, emission scenarios and other uncertainty sources.

Massah Bavani et al. (2011) appraised climate change impact on the Aidoghmoush basin, Iran, for the period 2040-2069, using the A2 emission scenario and HadCM3 atmospheric model. They found that rainfall would change around 30-40 percent in the future. Babaian et al. (2009) assessed climate change impact in Iran and used Echo-G output data based on the A1 emission scenario for 43 synoptic stations. Their results illustrated a 9% reduction in total rainfall. However, they also found that heavy and very heavy rainfall would increase between 13% and 39% for the period 2010-2039 and concluded more rainstorm and heavier rainfall in future decades for Iran. Goodarzi et al. (2011) investigated the impact of climate change on rainfall in an arid region of Yazd, Iran. They used CGCM3 output data based on the A2 emission scenario and showed an increase would happen in rainfall in December, January, February, and April and a decrease in other months in the period of 2010-2039 based on the 1982- 2008 period. Thus, future climate changes are generally believed to lead to an increase in climate variability and the frequency and intensity of extreme events.

Kim et al., (2002) claim that the evaluation of extreme events needs either the use of regional climate models, high-resolution Global Climate Models, or downscaling data to a smaller time scale to

improve the analysis and accuracy of GCM results. The use of fewer climate projections in model simulations may also restrict the full range of possible scenarios and increase the uncertainty of modeled future climate change conditions.

Some studies have utilized the multi-model, multi-scenario approaches, or both, along with a high-resolution model simulation of probability of extreme events. When comparing different uncertainty sources for climate change impacts on the flood frequency in England, Leanna et al., (2009) found that the uncertainty linked with the GCM is the prime source of uncertainty. In this study, we aimed at estimating the potential impacts of climate change and identifying rainfall characteristics when assessing the impact of climate change on rainfall indices in the Kooshkabad watershed for two future periods 2020-2045 and 2045-2065 under the three GCMs and two emission scenarios namely medium A1B and lower forcing B1 and RCP2.5, RCP8.5 scenarios. List of CMIP3 and CMIP5 global climate models used in this study are presented in Table1. The contents of this paper are organized as follows.

We first introduce the study area and data. Then we discuss the methodologies including stochastic weather generator LARS-WG and change factor for generating daily rainfall CIMP5 model data downscaled for the future. We then analyze impacts of climate change on rainfall indices and frequency at three rainfall gauge stations.

Materials and methods

Study area

The study area covers 2400 km2 in Kooshkabad Watershed, located in Hamedan Province of Iran between 34°48′ to 34°85′N and 48°26′ to 48°67′E. Figure 2 gives an overview of the study area location.

Table 1. List of CMIP3 and CMIP5 global climate models used in this study

Research center	Country	Global climate model	Model acronym	Grid resolution	Emissions scenarios	Source
National Institute for nvironmental	Japan	MRI-CGCM2.3.2	MIHR	2.8 × 2.8°	SRA1B, SRB1B	K-1 Model Developers (2004) Studies
Max-Planck Institute for Meteorology	Germany	ECHAM5-OM MPEH5	MPEH5	1.9 × 1.9°	SRA1B, SRA2, SRB1B	Roeckner et al. (1996)
Goddard Institute for Space Studies	USA	GISS-AOM	GIAOM	3 × 4°	SRA1B, SRB1B	Russell et al. (1995)
Max Planck Institute for Meteorology, GermanyMPI-	Germany	ESM-LR	MPI	1/875× 1/85°	RCP2.5, 8.5 scenario	Raddats et al. (2007)

The topography is rather complex, with elevation ranging from around 1750m to around 3570m. Annual rainfall shows substantial variations within the catchment, ranging from approximately 250mm to 750mm, for the period 1983-2010. Maximum monthly rainfall at the study area occurs during March with an average of 56.65mm, whereas the minimum monthly rain is 0.38mm, observed in September.

The monthly minimum temperature equals −1.5◦C and occurs during February, whereas the monthly maximum temperature is +22.5C, and happens in July. The climate of the study area is semiarid with dry summer, humid and cold winter and humid spring respectively.

Methodology

Climate scenarios approach

We analyzed climate simulations of the 20th and 21st century performed by models CMIP3 and CMIP5 for rainfall indices estimation in the sub basin of Kooshkabad Watershed in Hamedan Province, Iran. The meteorological data was received from the HPMO Organization.

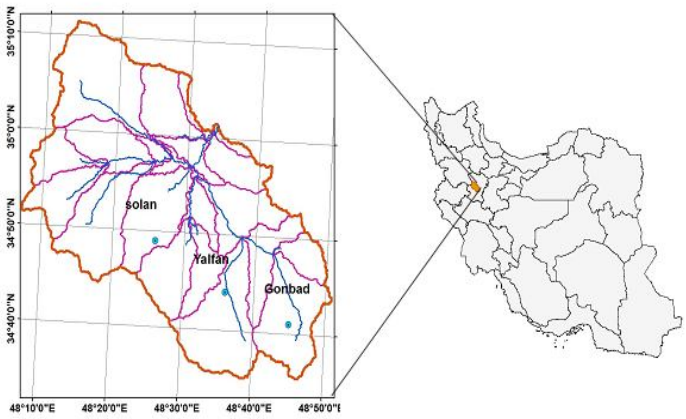

Figure 2. Study area location

However, our analyses were limited to three stations as only these stations had long and reliable data. Compared with the emission scenarios in CMIP3 and CMIP5, the representative concentration pathways (RCP) related to the radiative forcing are identified as new climate scenarios in CMIP5, and they include RCP2.6, RCP4.5, RCP6.0, and RCP8.5. So in this study, we mainly focused on the changes in extreme rainfall events in the study area at the end of the 21st century based on the CMIP3, A1b, and B1 emissions scenarios and CMIP5 models in the RCP2.5 (medium radiative forcing scenario) and RCP8.5 (high radiative forcing scenario) scenarios. The daily rainfall outputs from one CMIP5 model for the period 2020–2064 in the RCP2.5 and RCP8.5 scenarios and outputs from three CMIP3 models were used. In the low emissions scenario (RCP2.6), the atmospheric CO2 concentration peaks at just over 440 ppm in 2050 and then goes down to 420 ppm by the year 2100. Methane concentration culminates at just over 1770 ppb in 2010 and then reduces rapidly, reaching around 1250 ppb by 2100. The RCP2.6 scenario has total CO2 emissions similar to present-day levels until 2020 and then shows a sharp decline to zero carbon emissions by 2075.

The high emissions scenario (RCP8.5) is characterized by a progressive increase in atmospheric CO2 concentration over the twenty-first century, climaxing at 935 ppm in 2100. Methane also shows a very significant rise in the atmosphere under this scenario, peaking at 3750ppb in 2100. Total CO2 emissions increase from present-day values to a maximum of around 28 PgC yr21 in 2100. The CO2-equivalent concentration for greenhouse gases in the year 2100 is 475 ppm for the RCP2.6 scenario and over 1300 ppm for the RCP8.5 scenario. For each of the RCPs, two ensemble members are run.

We used some rainfall indices to compare the performances of the CMIP3 and CMIP5 in generating rainfall indices. Rainfall indices assessed in this study are: sum of wet days, simple rainfall intensity, very heavy rainfall days (count of days where RR $\geq$ 20 mm), maximum one-day rainfall and frequency. Data was downscaled with the statistical downscaling method, LARS-WG, change factor (CH) and, bias-corrected statistical method.

We analyzed the projected changes in daily precipitation, precipitation extremes and several precipitation indices. The output of three GCMs model (MPE5, GIOAM, MIHR) were downscaled using the LARS-WG model to generate daily rainfall for CIMP3. Also, the change factor method with change in mean and variance was used for generating daily rainfall in CIMP5 model data. The emission scenarios were medium A1B (700 ppm by 2100) and, lower forcing, B1 (550 ppm by 2100).

In all simulations, the time slices from 1983 to 2010 were considered as the reference period, and periods 2020–2030, 2046–2065, as a future scenario were extracted.

Downscaling approach

LARS-WG Technique

LARS-WG technique was developed in the UK by Dr, Mikhail Semenov as a tool for agricultural impact assessments (Racsko et al., 1991; Semenov and Porter, 1994; Semenov and Barrow, 1997). In two studies, LARS-WG was used for the simulation of weather data at a single meteorological station because of its capability of simulating extreme weather events (Semenov et al., 1998; Semenov, 2008). The model uses a time series of rainfall, max and min temperatures, and solar radiation as inputs.

LARS-WG analyzes the observed rainfall series to determine the statistics of wet-day occurrence and mean daily rainfall. In the process, semi-empirical distributions are redeveloped to simulate wet and dry-spell length with daily rainfall amount conditional on the spell length (Semenov and Barrow, 2002; Khan et al., 2006; Hashmi et al., 2011). LARS-WG is used to generate synthetic historical climate data as well as data for each AOGCM and emissions scenario. In the process, a stochastic weather generator is used to generate daily rainfall patterns that are statistically similar to the observed patterns.After generating future climate change data using LARS-WG for stations, F-Test is applied to compare the distributions of the observed and simulated rainfall indices during the baseline period (1983-2010).

Change factor approach

The change factor approach is a method that makes the output of GCMs useful for catchment-scale analysis and hydrological modeling. The method is based on the use of a change factor, the ratio between a mean value in the future and historical run. This factor is then applied to the observed time series to transform this series set into a time series that is representative of the future climate. The future daily rainfall *(PFut,d)* is obtained by multiplying the observed daily series *(PObs,d)* by the ratio of the mean monthly rainfall value for the GCM scenario series *(PSce,m)* to the control series *(PCon,m)*, shown below.

$$P\,Fut\,d = PObs\,d \times PSce\,m / pCon\,m$$

We used changes in mean and variance suggested by Leander and Buishand (2007) for downscaling outputs of CMIP5 data. This method is based on a non-linear correction approach and corrects the mean and variance of the observed time series using the CF of the mean and variance.

Results

Effects of climate change o monthly rainfall

In this section, the impact of climate change on monthly rainfall is briefly analyzed for the period 2045-2065 (2046–2065) based on three GCMs models and emission scenarios, A1B and B1. For 2045-2065 period, the synthetic daily rainfall data are generated by LARS-WG.

Monthly rainfalls from different GCMs and emission scenarios are extracted from the output of LARS-WG and calculated for different stations. Figure 2(a)–(c) shows the relative changes of monthly rainfall compared with GCM projections during the baseline period (1983– 010) under the three different scenarios in the region. Figure 2(a) showed that the relative change in monthly rainfall varies under the three GCMs models (MPE5, GIOAM, MIHR) for scenario A1B for the period 2045- 2065. The Range of relative change in January varies from -7% to -17.4% and relative change from January to June and November, December ranges from 17.2% to -32%.

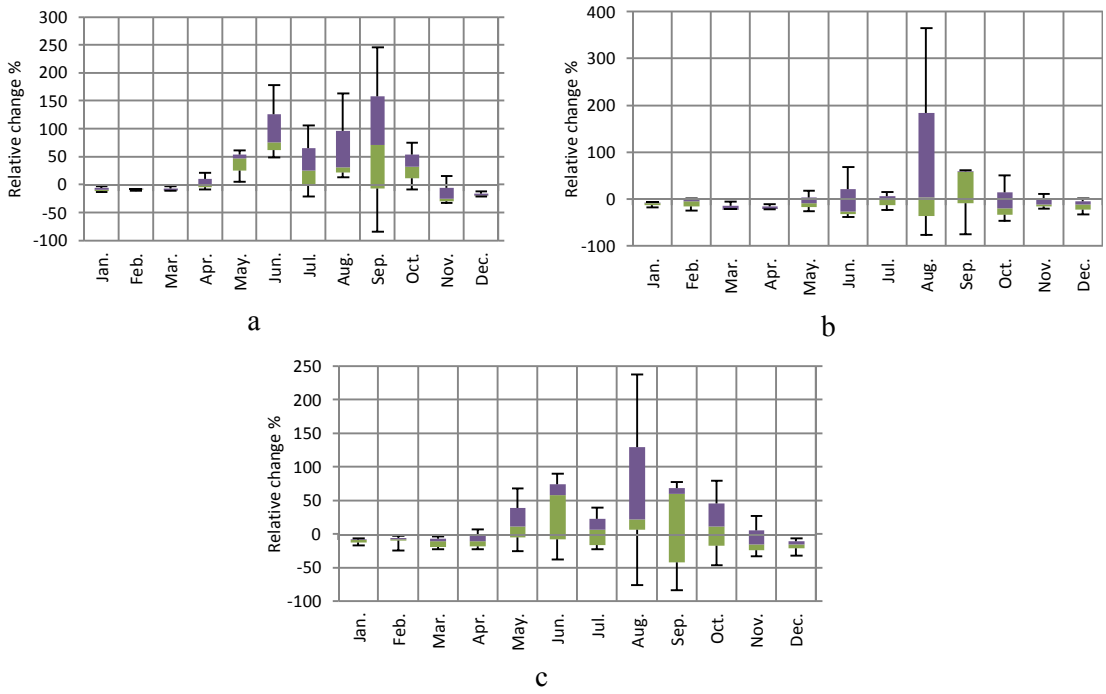

Figure 2. (a)–(c) Boxplot graphs of relative changes of monthly precipitation for the future 2045-2065 under the three GCMs models (MPE5, GIOAM, MIHR) under scenario A1B (a) scenario B1 (b) and combined scenario A1B & B1 (c).

We observe that monthly rainfall decreases in most months under the three GCMs scenario B1. Figure 3(b) show that the range of relative change in January varies from –2.5% to -13.9% and we see a five month decrease in rainfall while in other months an increase in monthly rainfall is seen with large uncertainty. We found that in the three GCMs models, relative change in rainfall varies under emission scenarios, A1B and B1. In the emission scenario A1B the decrease in monthly rainfall is more than that in scenario B1. Using a combination of the models, in Figure 2(c) we see that rainfall increases slightly with considerable uncertainty in the warm period and decreases in the cold period respectively for a future period (2046–2065). Hence, results showed decrease in rainfall in January, February, March, April, November and December with the lowest uncertainty and increase in rainfall in May, June and August with the highest uncertainty.

Table 2. RMSE and EF errors for rainfall indices and probability distribution function in the stations

Parameters	Distributions	solan		yalfan		gonbad	
		RMSE	EF	RMSE	EF	RMSE	EF
Simple Daily Intensity Index	Normal	0.33	0.95	0.17	0.97	0.31	0.93
	Lognorm2par	0.38	0.94	0.19	0.96	0.27	0.95
	Lognorm3par	0.38	0.94	0.19	0.96	0.25	0.95
	Pearson typ3	0.32	0.96	0.17	0.97	0.25	0.95
	Logpearson typ3	*0.3*	*0.96*	*0.15*	*0.97*	0.25	0.95
	Gambel1	0.49	0.9	0.26	0.92	*0.22*	*0.96*

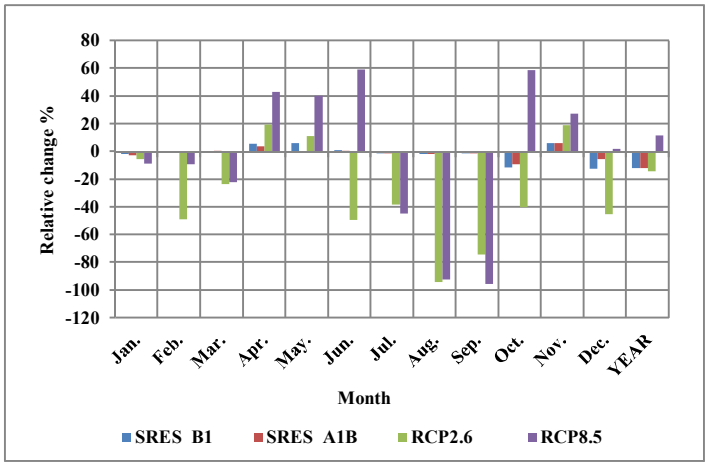

Figure 3. Comparison of CMIP3 and CMIP5 models of average monthly precipitation for 2020–2045 period based on reference period (1983–2010).

The relative change in monthly rainfall varies under the three GCMs models (MPE5, GIOAM, MIHR) scenario A1B, B1 and, RCP2.6 RCP8.5 for the future period 2020-2045, as shown in Figure3.

Range of relative change in January varies from -8.5% to -1.9% and corresponding change in all month ranges from -95.4% in September to 59% in June under the three GCMs models (MPE5, GIOAM, MIHR) scenario A1B, B1 and RCP2.6 RCP8.5 for the future period 2020-2045. The greatest relative change in monthly rainfall was seen in the warm season under the RCP2.6 RCP8.5 scenarios. The relative change of average monthly rainfall is predicted to decrease in winter under the CIMP3 and CIMP5 models for 2020–2045 period. In Figure 3, it also can be observed that the monthly rainfall decreases in most of the months, and the relative change of annual rainfall varies from 10.92% under RCP2.6 to -16.04% in SRES A1B, shown in Figure 4.

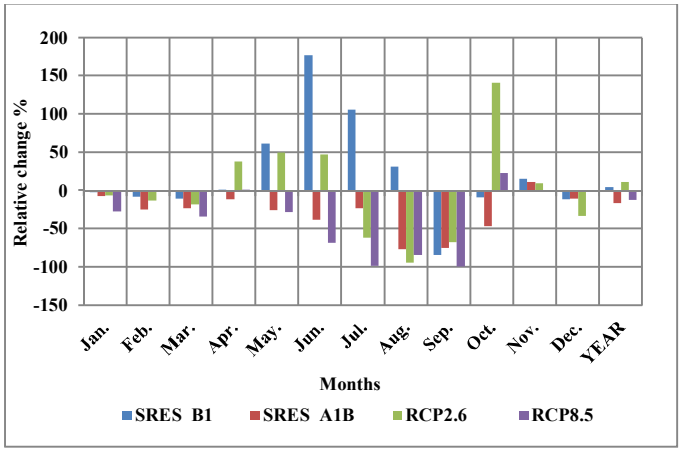

Figure 4. Comparison of CMIP3 and CMIP5 models of average monthly precipitation for 2046-2065 period based on reference period 1983–2010.

Rainfall indices analysis by fitting a distribution

After we made sure that the two data series follow the same continuous distribution, we compared the simulated rainfall indices and observed data sets. For assessing the frequency and return period and comparing the two data series, it was necessary to select the best probability distribution function for frequency analysis of rainfall indices. Table2 shows the extracted and computed best distribution functions for

simulated rainfall indices. Based on RMSE and EF methods, the best probability distribution function was selected. Results showed that most of the data followed the Log Pearson Type III. In Table3, we show the observed and simulated data for different return periods at three stations using log Pearson Type III probability distribution function. We see that the errors are small for most of the return periods and indices.

Table.3 Rainfall indices estimated for different return periods in the Yalfan station

Parameters	R Period	100	50	25	10	5
Simple Daily Intensity Index	Observed	9.4	9.2	8.9	8.5	8
	Simulated	9.8	9.5	9.1	8.6	8.1
	Error	4.4	3.4	2.5	1.3	0.2
Maximum one-Day Rainfall	Observed	69.5	62.9	56.4	47.6	40.7
	Simulated	63.4	58.5	53.5	46.4	40.4
	Error	8.9	7	5.1	2.6	0.7
Heavy Rainfall Days ≥20	Observed	8.4	7.3	6.3	4.9	3.8
	Simulated	7.7	6.8	5.8	4.5	3.5
	Error	7.9	7.9	7.8	8.1	8.7

After analyzing frequency distribution, Log Pearson Type III distribution was selected as the best frequency distribution and fitted to the data for CMIP3 and CMIP5 models.

Assessment of climate change impacts on rainfall indices

CMIP3 and CMIP5 data models were used to analyze daily climate model data sets over the study area. For CMIP3, we chose the GIOAM, MIHR, CMIP3 models, which provide the rainfall indices under the historical period 1983–2010.

For evaluating the relative change in the three GCMs models and scenarios, 50y return period was computed and compared with the base period 1983-2010.

The relative changes of the calculated 50y return period for rainfall indices were estimated and showed against the base period using the Log Pearson Type III probability distribution function in Figures 5, 6 and, 7(a)–(d). Here we focused on the analysis of the possible future changes in 50y design rainfall depths based on different GCMs and scenarios.

Figure 5(a) and (b) show relative changes in 50y simple daily intensity, decreasing in Gonbad and, increasing in Solan and Yalfan stations for the future 2020-2045 for scenarios A1B and B1. However, under the scenario A1B, Figure 5(c) shows increase only in Solan and decrease in Gonbad and solan, while under scenario B1 (d) we see an increase in Solan and Yalfan, and a decrease in Gonbad for future 2045-2065 with respect to the base period. Figure 6(a)-(d) depicts relative changes in 50y maximum one-day rainfall for the future 2045-2065 for scenario A1B (a) which shows decrease in rainfall under scenario A1B (c) and increase in Solan and yalfan under scenario B1 (d). Figure 7 (a)–(d) demonstrates the relative changes in 50y heavy rainfall days ≥20. For the future 2045-2065 for scenario A1B (c) heavy rainfall days decrease in Yalfan while for scenario B1(d), this index increases.

The results showed that the three indices in Solan and Yalfan stations for both future periods decrease under scenario A1B and increase under scenario B1.

Figure 6 (a)–(b) compares the relative changes in 50y maximum one-day rainfall for the future 2020-2045 for scenario A1B (a), scenario B1(b) and the future period 2045-2065 for scenario A1B (c) scenario B 1(d) under the three GCMs models (MPE5, GIOAM, MIHR). The results showed increase in 50y maximum one-day rainfall for the future 2045-2065.

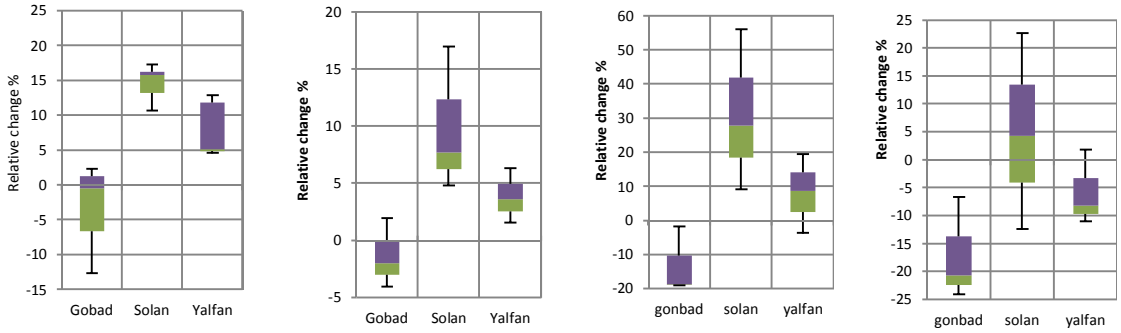

Figure 5. (a)–(d) boxplot graphs of elative changes in 50y simple daily intensity index for the future 2020-2045 for scenario A1B (a), scenario B1(b) and the future period 2045-2065 for scenario A1B (c) scenario B1(d) under the three GCMs models CMIP3 (MPE5, GIOAM , MIHR).

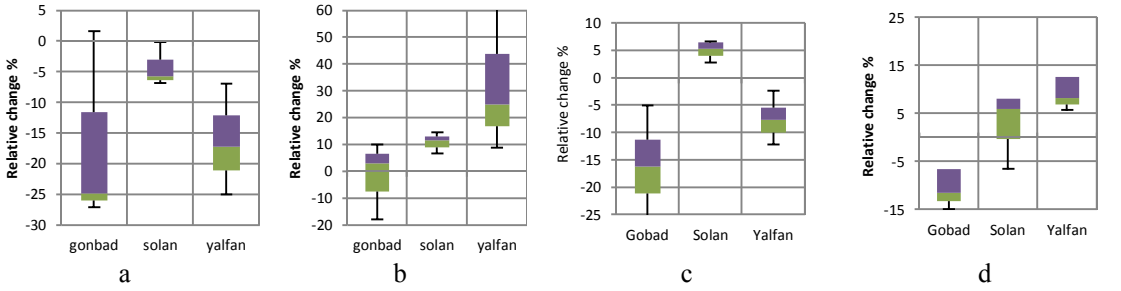

Figure 6. (a)–(d) boxplot graphs of elative changes in 50y maximum one-day rainfall for the future 2020-2045 for scenario A1B (a), scenario B1(b) and 2045-2065 for scenario A1B (c) scenario B1(d) under the three GCMs model (MPE5, GIOAM, MIHR).

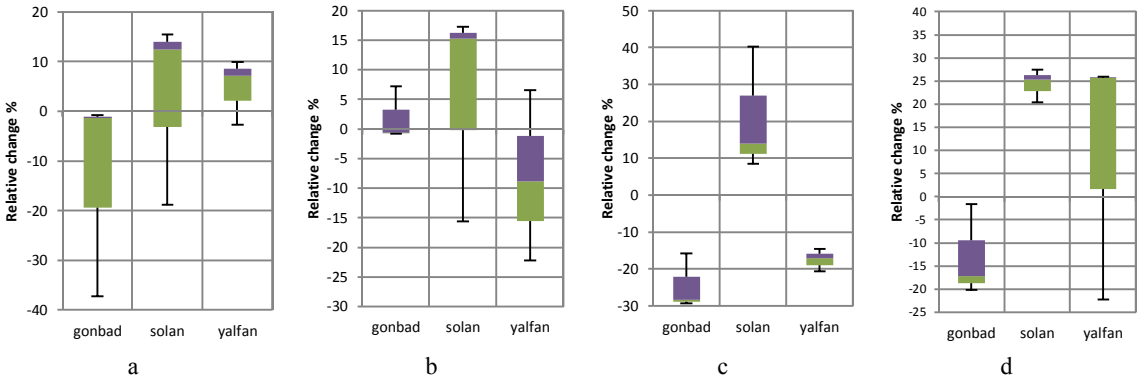

Figure 7. (a)-(d) boxplots of relative changes in 50y heavy rainfall days ≥20 for the future 2020-2045 for scenario A1B (a), scenario B1(b) and future period 2045-2065 for scenario A1B (c), B1(d) under the three GCMs models (MPE5, GIOAM, MIHR).

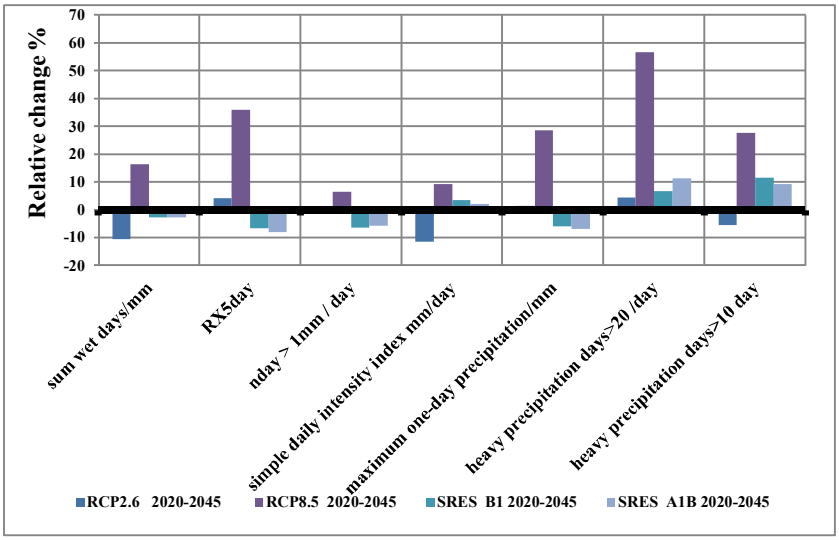

Figure 8. Relative changes in rainfall indices for scenarios A1B, B1and RCP2.5 and RCP8.5 scenarios for the future 2020-2045.

Rainfall indices of sum of wet days, number of days> 1mm and, maximum one-day rainfall are projected to decrease under the scenarios B1, A1B and sum of wet days, simple daily intensity and, heavy precipitation days >10 decrease under the RCP2.6. All of the rainfall indices were expected to increase in RCP8.5 scenarios for the future 2020-2045 as shown in Figure 8.

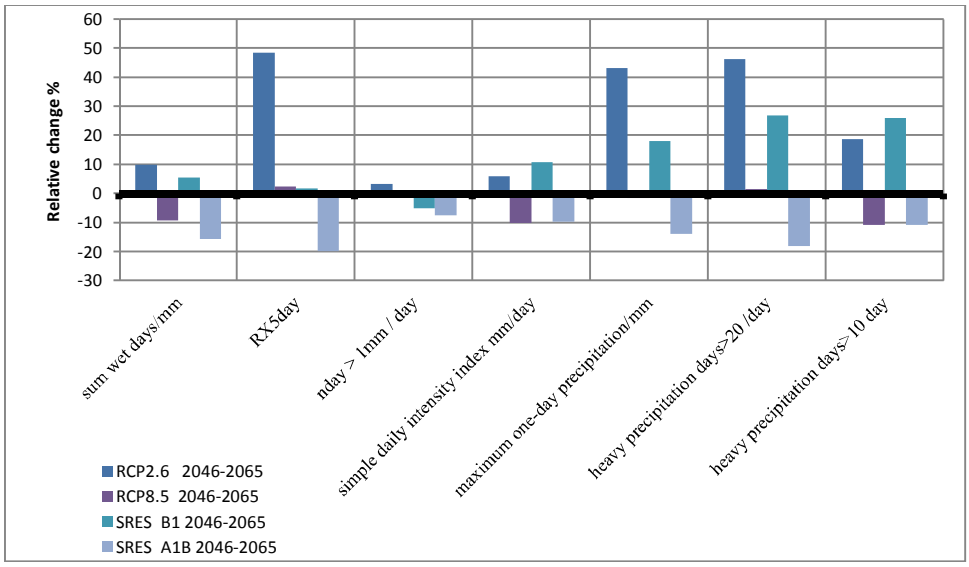

Figure 9. Relative changes in rainfall indices for scenarios A1B, B1 and RCP2.5 and RCP8.5 for the future 2046-2065.

Rainfall indices show considerable changes toward the end of the 21st century. Analysis of rainfall indices shows that except scenario RCP2.6 and SRES A1B, the predictions show a decrease in the indices as we progress toward the end of the 21st century. This indicates significant decreases in the sum of wet days, number of days> 1mm, simple daily intensity and, heavy precipitation days (Figure 8a). Also, rainfall indices for RCP8.5 scenarios and SRES A1B are predicted to increase toward the end of the 21st century. All of the Rainfall indices were expected to decrease

under the SRES A1B for the future 2046-2065, while they were predicted to increase in RCP2.6 scenarios as shown in Figure 9.

Discussion

I conclude that uncertainties exist in CMIP3 and CMIP5 models for the rainfall indices. Figures 5, 6 and 10 show various return periods for emission scenarios CMIP3 models for the sum of wet days, heavy rainfall, maximum one-day rainfall and, simple daily intensity index. The CMIP3 models and emission scenarios with various return periods predict considerable variation in (a) the sum of wet days, (b) simple daily intensity index, (c) maximum one-day rainfall and, (d) heavy rainfall days ≥20 for the period 2045-2056. Analysis of rainfall indices shows that except for other rainfall indices, heavy rainfall days ≥20mm is predicted to be highest under the CMIP3 and CMIP5 models except for RCP2.6. It could be observed that the return period of (a) simple daily intensity index, (b) maximum one-day rainfall under SRES B1 and RCP2.6 scenarios based on CMIP3, CMIP5 models are predicted to increase for 2045- 2056 based on the observed period 1983-2010, (Fig. 9). However, the return period of (a) sum of wet days, (b) simple daily intensity index and, (c) heavy rainfall days ≥20 under the SRES A1B and RCP8.5 scenarios based on CMIP3 and CMIP5 were predicted to increase toward the end of the 21st century.

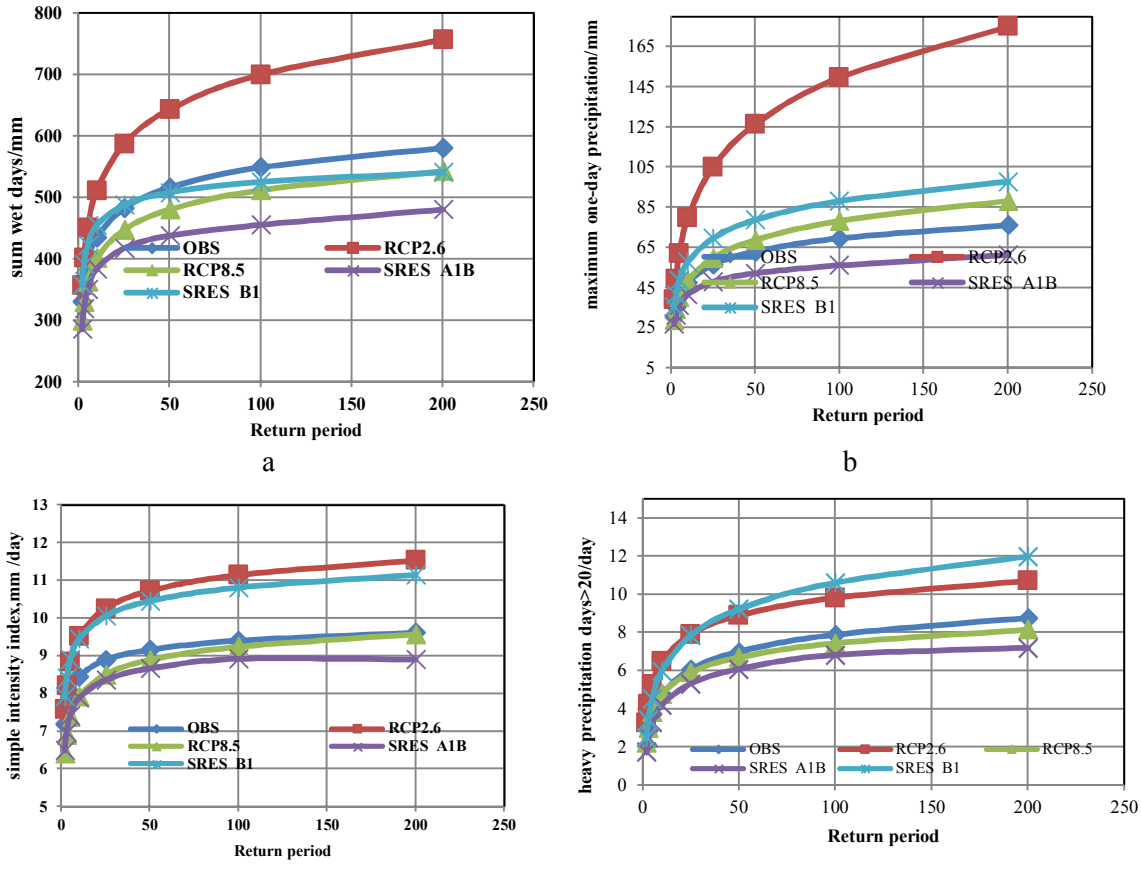

Figure 10. (a)–(d). Various return periods under the scenarios A1B, B1 and RCP2.5 and RCP8.5 scenarios for the future 2046-2065 for (a) sum of wet days, (b) simple daily intensity, (c) maximum one-day rainfall and (d) heavy rainfall days > 20 index.

A critical assessment of the impact of climate change on rainfall indices is the uncertainty that originate from different sources. These sources include future

greenhouse gas emissions, GCMs, downscaling methods, impact analysis models and parameters and so on (Yue-Ping Xu, et al., 2012). In this study, CMIP3, CMIP5 models and emission scenarios have been used.

Also, to investigate the impact of climate change on extreme rainfall, only one downscaling approach and one probability function (log Pearson Type III probability function) have been used. So, different probabilities bring about large uncertainties in the extrapolation of extreme rainfalls for return periods. Based on our current knowledge, this applies to projected changes in rainfall indices over the study area. Our focus in this paper was on the projected future changes in total precipitation and the related indices. Nevertheless, it is of utmost importance to also assess the ability of the different models to simulate the observed precipitation characteristics in the region.

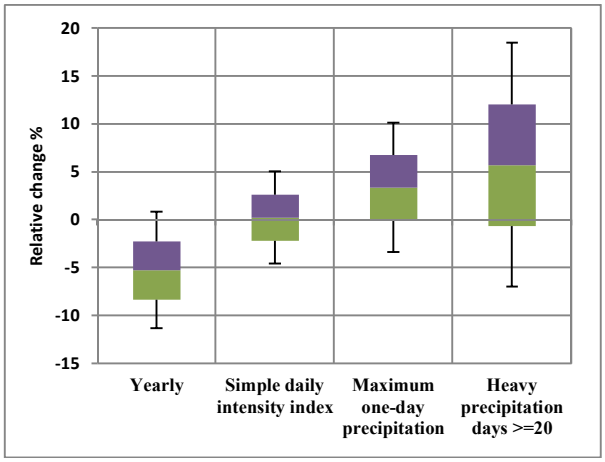

Figure 11. Boxplots of relative changes comparing observed period (1983-2010) with GCMs model under emission scenarios A1B and B1 for the future period 2045-2065.

Figure 11 provides a boxplot of relative changes for GCMs model under emission scenarios A1B and B1. This figure shows that, although the annual rainfall decreases in the study area, the indices of heavy rainfall days≥20, maximum one-day rainfall and simple daily intensity index increase for the future period 2045-2065 based on the observed period.

Conclusion

I used daily precipitation output of a large set of global and downscaled climate change projections available for a historical period and two future periods for several emission scenarios to project changes in future precipitation and evaluate extremes over Kooshkabad Watershed, Hamedan Province, west of Iran based on CMIP3, CMIP5 models. This study revealed the noticeable changes due to climate changes in the rainfall indices over the study area. Results showed that the monthly rainfall decreased in January, February, March, April, November and, December, with the lowest uncertainty and increase in rainfall in May, and June and the highest uncertainty in August. In general, a critical result of this study is the increase of rainfall indices under the most CMIP3, CMIP5 models and scenario B1 while the reverse was found for the emission scenario A1B. These findings show the difficulty with which water resources managers and planners are faced with when making decision under such considerable uncertainty in climate change. However, this does not make us needless of such investigations of rainfall characteristics for future climate conditions.

Analysis of return period for (a) heavy rainfall days with ≥ 20, (b) maximum one-day rainfall and (c) simple daily intensity index showed significant decrease under SRES A1B, RCP8.5 scenarios and, increase under SRES B1, RCP8.5 for CMIP3,

CMIP5 models and scenarios over the study area. Results showed that the annual rainfall depth decrease under the three GCMs models for scenario A1B was 11.8% and for scenario B1 was 1.44% for the future period 2045-2065. However, heavy rainfall days ≥20 decreased by 8.14% under the scenario A1B and increased by 13.7% under the B1 scenario. We showed that although relative annual changes decreased for GCMs models under emission scenarios A1B and B1, however, slight increase was likely in heavy rainfall days ≥20, maximum one-day rainfall and simple daily intensity index in the study area.

Future work should consider the uncertainties involved in climate change impact analysis on rainfall characteristics for downscaling methods that use regional climate models (RCMs) and statistical downscaling, change factor, change factor quantile mapping, and SDSM.

Acknowledgements
The authors thank the meteorological Organization of Hamedan Province and Research Center of Agriculture of Hamedan (RCAH) for providing meteorological data of the study area.

References

Albert, M.G., Klein Tank, Francis, Zwiers, W., and Xuebin Zhang, 2009 nalysis of extremes in a changing climate in support of informed decisions for adaptation. Climate Data and Monitoring, World Meteorological Organization. WCDMP-No. 72.

Andreas, H., Fahad, S., and Daniela, J, 2013. Assessing the robustness of projected precipitation changes over central Africa based on a multitude of global and regional climate projections. Climatic Change, DOI 10.1007/s10584-013-0863-8.

Ahmadi, L., Moridi, A., and Kakaei, E. 2014–A case study. Journal of Earth System Science Volume 123. The Effects of Climate Change on Extreme Rainfall Events in the Upper Thames River Basin: A Comparison of Downscaling Approaches.

Babaian. A. 2009. studied climate change impact in Iran in 2010-2039 with downscaling GCM model of ECO-G data. Journal of geography, 16: 135-152.

Beijing, China Wilby RL, Harris I. 2006. A framework for assessing uncertainties in climate change impacts: low-flow scenarios for the River Thames, UK. Water Resources Research 42, W02419.DOI:10.1029/2005WR004065.

Botao, Z., Qiuzi, H., Ying, X., and Lianchun, S., Xuebin, Z, 2014. Projected Changes in Temperature and Precipitation Extremes in China by the CMIP5 Multi-model Ensembles. American Meteorological Society, 27, 6591-6611.

Brown, P.J., Bradley, R.S., and Keimig, F.T. 2010. Changes in extreme climate indices for the northeastern United States. Journal of Climate, 23(24), 6555-6572.

Chen, H.P. 2013: Projected change in extreme rainfall events in China by the end of the 21st century using CMIP5 models, Chinies Science Bulltin, 58, 1462–1472.

Chen, J., Brissette, F.P., and Leconte, R. 2011. Uncertainty of the downscaling method in quantifying the impact of climate change on hydrology. Journal of Hydrology, 401(3–4), 192–202. DOI: 10.1016/j.jhydrol.2011.02.020.

Chen, S.T., Yu, P.S., and Tang, Y.H. 2010. Statistical downscaling of daily rainfall using support vector machines and multivariate analysis. Journal of Hydrology, 385, 13-22.

Chen, X.C., Y., Xu, C.H., Xu, et al. 2014. Assessment of precipitation simulations in China by CMIP5 multi-model, Advanced Climate Change Research, 10(3), 217–225.

Dong, S.Y., Xu, Y., and B.T. Zhou, et al. 2014: Projected risk of extreme heat in China based on CMIP5 models, Advanced Climate Change Research,10(5), 365–369.

Eemenov, M.A., and Brooks, R.J. 1999. Spatial interpolation of the LARS-WG stochastic weather generator in Great Britain. Climate Research, 11, 137–148.

Eum, H. I., and Simonovic, S.P. 2012. Assessment of variability of extreme climate events for the Upper Thames Basin in Canada. Hydrological Processes, 26, 485-499.

Fahad Saeed, Andreas Haensler, Torsten Weber, Stefan Hagemann and Daniela J. 2013. Representation of Extreme Precipitation Events Leading to Opposite Climate Change Signals over the Congo Basin. Atmosphere, 4, 254-271.

Fowler, H.J., and Kilsby, C.G. 2003. extreme rainfall. Geophysical Research Letters Vol. 30, No. 13, 1720, DOI: 10.1029 2003 GL 017327, 2003. Implications of changes in seasonal and annual.

Hashmi, M.Z., Shamseldin, A.Y., and Melville, B.W. 2011. Comparison of SDSM and LARS-WG for simulation and downscaling of extreme rainfall events in a watershed. Stochastic Environmental Research and Risk Assessment, 25, 475-484.

Hu, Y., Maskey, S., and Uhlenbrook, S. 2012. Trends in temperature and rainfall extremes in the Yellow River source region, China. Climatic Change, 110, 403-429.

IPCC, Intergovernmental Panel on Climate Change, 2007. Fourth Assessment Report, Climate Change.

Jeong, D.I., St-Hilaire, A.T., Ouarda, B.M.J., and Gachon, P. 2012. CGCM3 predictors used for daily temperature and rainfall downscaling in Southern Que ´bec, Canada. Theoretical and Applied Climatology, 107, 389-406.

Jie Chen, François P., and Brissette, 2011. Uncertainty of the downscaling method in quantifying the impact of climate change on hydrology Journal of Hydrology, 401,190–202.

Jones, P.D., and Reid, P.A. 2001. Assessing future changes in extreme rainfall over Britain using regional climate model integrations. International Journal of Climatology, 21, 1337–1356. DOI: 10.1002/ joc.677.

Kay, A. L., Davies, H.N., Bell, V.A., and Jones, R.G. 2009. Comparison of uncertainty sources for climate change impacts: flood frequency in England.

Khan, M.S., Coulibaly, P., and Dibike, Y. 2006. Uncertainty analysis of statistical downscaling methods. Journal of Hydrology, 319, 357–382.

Leanna, M.M. King, Sarah Irwin, Rubaiyaarwar. 2014.Assessment of climate change impacts on rainfall using large scale climate variables and downscaling. Canadian Water Resources Journal / Revue Canadienne des Ressource shydriques, 37, 3, 253-274.

Mailhot, A., Duchesne, S., Caya, D., and Talbot, G. 2007. Assessment of future change in intensity–duration–frequency (IDF) curves for Southern Quebec using the Canadian Regional Climate Model (CRCM). Journal of Hydrology, 347,197–210.

Massahbavani, A., and Sadatashofteh, P. 2010. Impact of climate change on maximum discharges: Case study: Aidoghmoosh watershed, East Azerbaijan, ran. Iranian Journal of Agricultural Science and Technology and Natural Resources, 53, 25-39.

Manville, M., Brissette F., and Leconte R. 2008. Uncertainty of the impact of climate change on the hydrology of a Nordic watershed. Journal of Hydrology, 358, 70–83.

Mary W. 2004. Simulation of the variability and extremes of daily rainfall during the Indian summer monsoon for present and future times in a global time-slice experiment. Climate Dynamics, 22, 183–204.

Nazaripouya, H., Kardavany P., and Faraji, A. 2016. Assessing Climate Change Impacts on Hydro-Climatic Parameters in the Dam Basin of Ekbatan, Hamedan. Iranian Journal of Ecohydrology. 3, 181-194.

Pourtouiserkani, A., and Rakhshandehroo, H. 2014. Investigating climate change impact on extreme rainfall events Case study: Chenar-R basin, Fars, Iran. Scientia Iranica, 21(3), 525-533.

Schoof, J.T. 2012. Scale issues in the development of future rainfall scenarios. Journal of Contemporary Water Research and Education, 147, 8-16.

Semenov, M.A. 2008. Simulation of extreme weather events by a stochastic weather generator. Climate Research, 35, 203–212.

Semenov, M.A., and Stratonovitch, P. 2010. Use of multi-model ensembles from global climate models for assessment of climate change impacts. Climate Research, 40(1), 1–14.

Semenov, M.A., Brooks, R.J., Barrow, E.M., and Richardson, C.W. 1998. Comparison of the WGEN and LARS-WG stochastic weather generators in diverse climates. Climate Research, 10, 95–107.

Seree, S. 2015. Studied assessment of CMIP3-CMIP5 climate model precipitation projection and implication of flood vulnerability of Bangkok. American Journal of Climate Change, 4, 140-162.

Solaiman, T., King, L., and Simonovic, S.P. 2010. Extreme rainfall vulnerability in the Upper Thames River basin: Uncertainty in climate model projections. International Journal of Climatology, 31, 2350-2364.

Tomozeiu, R., Cacciamani, C., Pavan, V., Morgillo, A., and Busuioc, A. 2007. Climate change scenarios for surface temperature in Emilia-Romagna (Italy) obtained using statistical downscaling models. Theoretical and Applied Climatology, 90, 25-47.

Von Stoch, H., Zorita, E., and Cubasch, U. 1993. Downscaling of global climate change estimates to regional scales: an application to Iberian rainfall in wintertime. Journal of Climate 6, 1161–1171.

Wetterhall, F., Halldin, S., and Xu, C.-Y. 2007. Seasonality properties off statistical-downscaling methods in central Sweden. Theoretical and Applied Climatology, 87, 123-137.

Wilks, D.S. 2010. Use of stochastic weather generators for rainfall downscaling. Wiley Interdisciplinary Reviews Climate Change, 1(6), 898–907.

Wilks, D.S. 1999. Multisite downscaling of daily rainfall with a stochastic weather generator. Climate Research, 11, 125–136.

Wilks, D.S. 2010. Use of stochastic weather generator for rainfall downscaling. Climate Change,1, 898–907.

Xu, C., Shen, X., and Xu, Y. 2007. An analysis of climate change in East Asia by using the IPCC AR4 simulations. Advances in Climate Change Research, 3(5), 287–292 (In Chinese).

Xu, Ying, Wu, Jie, Shi Ying, Zhou Bo-Tao, Li Rou-Ke and Wu, Jia 2015. Change in extreme Climate Events over China Based on CMIP5, Atmospheric and Oceanic Science Letters, 8, 4, 185-192.